

The Performance of PPO_{dm}-CNF Mixed Matrix Membrane for CO₂/CH₄ Separation

P. S. Murugiah, P. C. Oh* and K. K. Lau

CO₂ Research Centre (CO₂RES), Institute of Contaminant Management,
Department of Chemical Engineering, Universiti Teknologi PETRONAS,
Bandar Seri Iskandar, 32610 Seri Iskandar, Perak, Malaysia

* Email: peiching.oh@utp.edu.my

Phone: +6053687568; Fax: +6053656176

ABSTRACT

Mixed Matrix Membrane (MMM) is one of the most promising candidate among the available gas separation application for CO₂/CH₄ separation in natural gas industries. However, the fabrication of a defect-free MMM remains a challenge. For this work, a novel MMM was developed by incorporating carbon nanofibers (CNF) at different weight loadings into poly (2, 6-dimethyl-1, 4-phenylene oxide) (PPO_{dm}) polymer matrix via dry-phase inversion technique. CNF was purified with hydrogen peroxide prior to membrane fabrication. Approximately 178 % increment in the CO₂ permeability were attained at 3 wt% of CNF loading whereas the CO₂/CH₄ selectivity were increased by 53 % compared to pristine PPO_{dm} polymeric membrane. The smooth wall of CNF coupled with its larger pore diameter acted as a pathway and renders high gas permeability values. PPO_{dm} – 3 wt% CNF MMM exhibits improved morphology with no significant filler agglomeration on the polymer matrix. The TGA and DSC analysis showed that at 3 wt% of CNF loading, the thermal stability of the polymer chains was enhanced in which higher decomposition ($T_d = 425$ °C) and glass transition ($T_g = 210$ °C) temperatures were reported.

Keywords: Carbon nanofiber; poly (2, 6-dimethyl-1,4-phenylene oxide); mixed matrix membrane; CO₂ separation.

INTRODUCTION

Mixed matrix membrane (MMM) is considered to be the most researched topic in the last two decades for gas separation application. MMM is fabricated through the incorporation of uniformly dispersed filler particles on a continuous polymer matrix. MMM is also believed to combine the ease of processing of polymer matrix with the effective gas separation properties of filler particles [1]. An ideal MMM is expected to offer high selectivity values in separating CO₂ from CH₄ without sacrificing the polymeric membrane's permeability values. It is also expected to exhibit robust mechanical strength to sustain the long-term gas separation performance [2, 3]. Despite all the advantages of MMM, it is often challenging to fabricate a defect-free membrane for the industrial application. Therefore, to-date polymeric membranes are still dominating the gas separation processes in industries although it exhibits lower performance compared to MMM. The major limitation in MMM fabrication is the difficulty in achieving homogenous dispersion of inorganic fillers in the polymer continuous phase especially when the fillers are nano-sized [4]. Compared with the traditional micro-sized filler

particles, nano-sized particles at the same loading provides more interaction with the polymer matrix which disrupt more of the polymer chain packing and eventually enhance the molecular transport mechanism [5]. Therefore, in current practice, the nano-sized fillers particles are widely used for membrane fabrication process. However, the dispersibility of nano-sized fillers are comparatively poor, leading to higher tendency to agglomerate and form micro-sized clusters in polymer matrix [6]. Besides that, MMM also suffer from polymer-inorganic filler interface defects due to the major difference between polymer-inorganic particles properties together with the strong aggregation tendency of the filler particles.

It is worth mentioning that, most of these issues in MMM development could be resolved at the initial polymer-inorganic filler pair selection stage. Selection of the appropriate polymer matrix determine the basis of MMM gas permeability, whereas selection of appropriate filler particles determine the extent of separation performance and mechanical enhancement of the resultant membrane [7]. In the context of gas separation membrane development, the fillers particles could be divided into: (1) conventional fillers (i.e. zeolite, carbon molecular sieve, silica and metal oxide) and (2) alternative fillers (i.e. carbon nanotubes, layered silicate and metal organic framework). Conventional fillers and clay could considered as the most excessively researched fillers in this area as they possess some unique and individualistic properties which contribute to the robust performance of resultant membrane [8]. However, for the alternative fillers, only few works have been reported thus far. Therefore, for this work carbonaceous nanofillers are chosen to be used as the filler whereby among the carbonaceous nanofillers, only carbon nanotubes (CNTs) have been widely utilized in membrane fabrication process as they provide good perm-selectivity values with better mechanical strength [1]. However, CNT-based membranes are reported to encounter major agglomeration issues on the polymer matrix [9]. CNT's large aspect ratio, smaller size, strong π - π stacking effect and strong van der Waals forces between the graphene sheets in CNT has a major influence on its dispersibility. This phenomenon induces the formation of CNT agglomerates into the tight bundles or hollow ropes [10]. Thus, CNT needs to undergo pre-treatments which must be carried out in a very controlled condition to sustain the native properties of the filler particles [11, 12]. Due to limitations of CNT, an alternate filler which possesses similar properties is found.

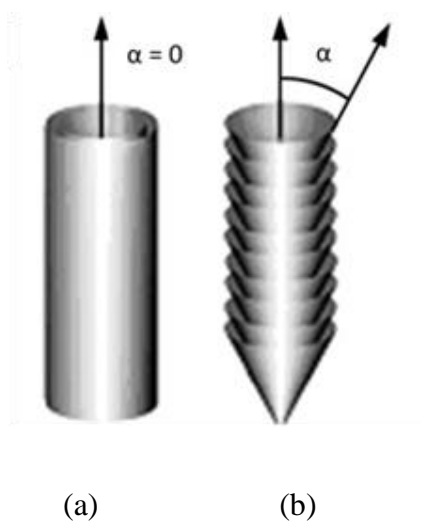


Figure 1. Schematic representation of (a) CNT and (b) CNF.

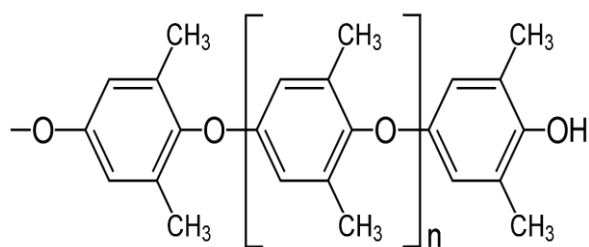


Figure 2. The chemical structure of PPO_{dm}.

Carbon nanofibers (CNF), is also a carbonaceous nanofiller which comprises of graphene sheets exhibits similar properties with CNT but hypothesized to display improved dispersion compared to CNT. CNF has a unique structure, known as stacked-up carbon nanotubes in which the graphene layers are curved at an angle, α to create stacks of nanocones as shown in Figure 1[13]. The graphene plane edges are exposed in CNF; hence it could easily interact with the polymer matrix without any complex functionalization process. In addition to that, CNF is also well-known for its high compatibility with most of the polymer processing techniques and exhibits similar robust mechanical and thermal properties as CNT. Therefore, CNF is selected to be the dispersed phase on poly (2, 6-dimethyl-1,4-phenylene oxide) (PPO_{dm}) continuous phase (Figure 2) for the MMM development. Thus, the main objective of this study is to synthesize and characterize PPO_{dm}-CNF MMM for CO₂/CH₄ separation. To the best of author's knowledge, no similar work has been reported for CNF-PPO_{dm} MMM in gas separation application.

EXPERIMENTAL SETUP

Materials

PPO_{dm} ($M_w=30,000$ g/mol) powder and solvent, chloroform (stabilized, purity ≥ 99.5 %) were purchased from Sigma Aldrich through Modern-Lab Chemical Sdn. Bhd. The CNF (average diameter of 200-600 nm, lengths ranging from 5-50 μ m, purity >70 %) was purchased from Suzhou Hengqiu Graphene Technology Co., Ltd. For CNF purification purpose, hydrogen peroxide aqueous solution, H₂O₂ (30 wt% stabilized) was purchased from Merck Sdn.Bhd.

CNF Purification

CNF is purified via a simple purification procedure as reported elsewhere [14] before incorporating it on the polymer matrix. Initially, 50 mg of CNF were introduced into 300 ml of H₂O₂. The mixture was heated and refluxed at 90 °C for 40 h. Then, the mixture was cooled to room temperature, filtered and washed with distilled water for several times. The resultant CNF was dried at 50 °C for another 50 h.

Membrane Preparation

PPO_{dm}-CNF MMM were fabricated via dry phase inversion technique at 22 wt% of PPO_{dm}. Prior to casting, polymer and CNF were dried at 60 °C and 150 °C respectively for 24 h. Then, a specified amount of CNF (1, 3 and 5 wt%) were dispersed in a small amount of solvent and sonicated for 30 min. After sonication, polymer was gradually added into the suspension while stirring for the next 24 h at 60 °C. The dope solution was degassed for 4 h and left standing at room temperature overnight. Finally, the dope solution was cast on a clean glass plate at a gap setting of 150 μm and dried to remove all traces of residual solvent. Pristine PPO_{dm} membrane was fabricated via the same procedures without the addition of filler at initial stage.

Membrane Characterization

The morphology observation of CNF (before and after purification) was performed using Variable Pressure Field Emission Scanning Electron Microscope (VP-FESEM, Zeiss Supra 55 VP). The same VP-FESEM was used to analyze the cross-section morphology of all the resultant membranes with an accelerating voltage of 15kV. For cross-sectional morphology analysis, the membranes were fractured using liquid nitrogen, prior to scanning. The glass transition temperature (T_g) of membranes were measured with a Differential Scanning Calorimeter (DSC, TA instruments, Q2000) under N₂ flow in the temperature range of 50-400 °C at a heating rate of 10 °C/min. The thermal stability of the membranes (decomposition temperature (T_d)) were identified using Thermal Gravimetric Analyser (TGA, Perkin Elmer, STA 6000) from room temperature up to 850 °C under N₂ flow at a heating rate of 10 °C/min.

Gas Permeation Test

The gas permeability of the membranes was measured using pure CO₂ and CH₄ gases via conventional constant pressure/variable-volume method as described elsewhere [15]. The fabricated membranes were cut into a sphere shape with diameter of 1.50 cm and dried in a vacuum oven at 80°C for at least 1 hour before gas permeation test. The permeation test was carried out at room temperature with a fixed feed pressure, 3.5 bar. The gas flow rate was measured at steady state conditions. The gas permeability (P_i , Barrer, and 1 Barrer = 10⁻¹⁰ cm³ (STP) cm/ (cm² s cmHg)) is calculated using Eq.(1):

$$\frac{P_i}{l} = \frac{Q_i}{\Delta p_i A} \left(\frac{273.15}{T} \right) \quad (1)$$

where P_i/l is the permeance of membrane to a gas i (cm³ (STP)/cm² s cmHg), P is the permeability (cm³ (STP) cm /cm² s cmHg), l is the membrane thickness (cm), Q_i is the volumetric flow rate of gas i (cm³ (STP)/s), Δp_i is the partial pressure difference of gas i between the feed and permeate side (cmHg), A is the effective membrane area (cm²) and T is the experimental temperature (K). After the gas permeability of both gases were calculated the CO₂/CH₄ selectivity (α_{CO_2/CH_4}) was calculated from Eq. (2):

$$\alpha_{CO_2/CH_4} = \frac{P_{CO_2}}{P_{CH_4}} \quad (2)$$

The measurements were taken 5 times for each membrane sample and the average values were reported.

RESULTS AND DISCUSSION

The purification of CNF is very essential since the untreated CNF may contain various impurities such as amorphous carbon, incompletely grown carbon, catalytic metals and other carbon nanoparticles. These impurities need to be removed from the surface of CNF without damaging its structure [14]. After purification, the effect of hydrogen peroxide treatment on the morphology of filler particles was observed through FESEM images at a magnification of 25,000x and shown in Figure 3.

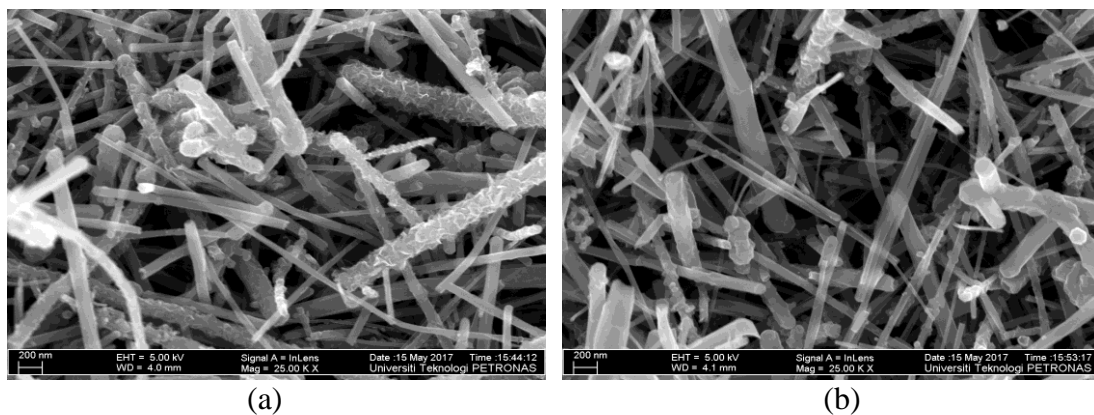


Figure 3. FESEM images of CNF (a) before and (b) after purification at magnification of 25,000x.

From Figure 3, it is observed that the diameter of CNF particles has significantly reduced after hydrogen peroxide treatment. The average diameter of the CNF particles before and after purification was found to be approximately 117 and 86 nm, respectively. Before purification, the carbonaceous impurities in Figure 3(a) were distributed entirely on the surface of CNF particles. These impurities might hinder the interaction of CNF with polymer chain during membrane formation and resulting in undesired filler agglomeration on polymer matrix. In addition to that, these impurities also could hinder the gas flow through the CNF-based membranes which eventually reduces the gas permeability values [16]. After purification, the amount of impurities on the CNF surface has reduced in a greater extent as depicted in Figure 3 (b). The hydrogen peroxide treatment also does not alter the native morphology of CNF [14]. Hence, this simple purification step was deemed effective as it only reduces the impurities stuck on the CNF structure without major morphological transformation.

After the CNF is purified, the membrane was fabricated via dry-phase inversion technique. The thermal degradation characteristics of the as-synthesized PPO_{dm}-CNF membranes were analyzed from the weight loss percentage vs. temperature plot (Figure 4). Very similar thermal profile was observed for all the membranes, regardless of the filler composition. Decomposition started at approximately 410 °C and continued until

460 °C. There was no significant weight loss observed before 410 °C whereby only one major weight loss step which referred to the main polymer chain and methyl group degradation could be noticed [17]. This corroborates the absence of residual solvent or trapped moisture remaining in the membrane. Furthermore, the MMMs also showed a huge weight loss of about 60% ± 5 between the temperature range of 410-460 °C. For this research work, the decomposition temperature, (T_d) was determined at 5% of sample weight loss (95 % of total weight is left) and presented in Table 1. The result obtained for pristine PPO_{dm} membrane was in good agreement with previous work reported by Yoshimune et.al. [18]. At 1 wt% CNF loading, the T_d was increased from 416 °C to 421°C, and further increased to 425 °C for 3 wt% CNF loading. This small increment (5-9 °C) might be contributed by polymer-filler interactions as well as the high thermal stability of CNF particles. The CNF particles able to absorb heat, offers a stabilizing effect against decomposition, inhibits the diffusion of degradation products from the bulk of polymer phase onto the gas phase and finally results in higher degradation temperature [19].

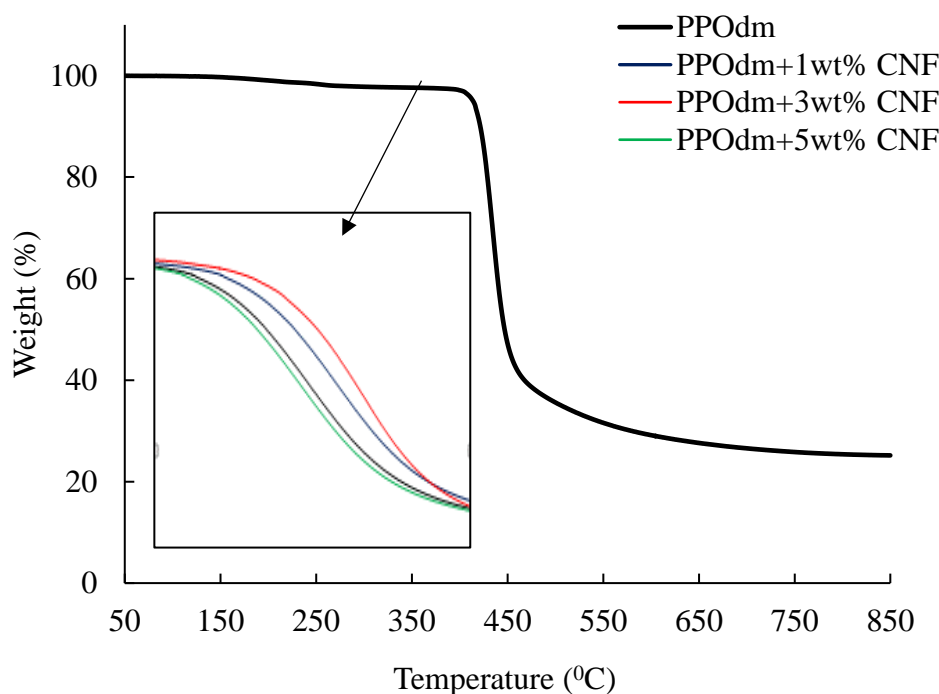


Figure 4. TGA curves of as-synthesized membranes at different filler concentration

Following that, the flexibility of the polymer chain was determined by measuring the glass transition temperature, T_g of membrane where the polymer changes from a hard, rigid and glassy material to soft and rubbery. The T_g values of the resultant membranes at different filler concentration was determined via DSC analysis and tabulated in Table 1. Similar trend was obtained, in which a drastic increment in the T_g value (about 12°C) could be observed after CNF was introduced to the polymer matrix. The highest T_g value was obtained at 3 wt% filler loading (210°C) which was 16°C higher than the T_g of pristine PPO_{dm} membrane. This increment in T_g was contributed by the constrained motion of polymer chains in MMMs due its interaction with the CNF particles as well as CNF entanglement within the polymer chain that causes polymer rigidification around the filler particles [20]. However, at 5 wt% filler loading both the T_d and T_g values were started to

decrease. This might be caused by the increase in polymer matrix free volume in the MMMs as the result of strong PPO_{dm}-CNF interaction as well as CNF agglomeration at higher loading [21]. Therefore, 3 wt% of CNF loading could be considered to be the optimum loading for CNF-based membrane fabrication.

Table 1. Thermal properties of the resultant membranes at different filler loading.

| Membrane | T_d (°C) | T_g (°C) |
|-------------------------------|------------|------------|
| Pristine PPO _{dm} | 416 | 194 |
| PPO _{dm} + 1 wt% CNF | 421 | 206 |
| PPO _{dm} + 3 wt% CNF | 425 | 210 |
| PPO _{dm} + 5 wt% CNF | 416 | 207 |

Moreover, the cross-sectional images of membrane were analyzed to investigate the degree of CNF dispersion within the polymer matrix and to study the polymer-filler interaction. All membranes possess an average thickness between 9–34 μm whereby 11.52 μm , 21.52 μm , 9.40 μm and 33.52 μm was measured for pristine membrane and MMM with 1, 3 and 5 wt% filler loading, respectively. From these values it could observe that, there was a reduction in the thickness of the resultant membrane at 3 wt% filler loading. This was likely to be attributed by strong adhesion between PPO_{dm}-CNF particles due to the densification of macromolecules, thus the macromolecules experience the tightest coiled conformation and eventually produces thinner layer of membrane. This tight macromolecular conformation also able to hinder pinhole formation on the membrane surface [22]. The cross-sectional image of the pristine PPO_{dm} membrane in Figure 5 (a) shows a dense, non-porous and homogenous structure in which the gas molecules were expected to diffuse through the membrane via solution-diffusion mechanism. Since CO₂ and CH₄ have smaller kinetic diameter difference, dense membranes are preferred compared to porous membrane for a highly selective gas separation process. Interestingly, after the filler particles were incorporated in the PPO_{dm} polymer matrix, the dense, non-porous structure of membrane remained as illustrated in Figure 5 (b) and (c). At 1 and 3 wt% filler loading, the CNF particles dispersed homogeneously on the polymer matrix. No significant voids or polymer-filler interfacial defects were observed from these images. Nevertheless, at 5 wt% CNF loading the dense structure of PPO_{dm} membrane has transformed to be wavy and the dispersion of CNF particles could not be clearly observed.

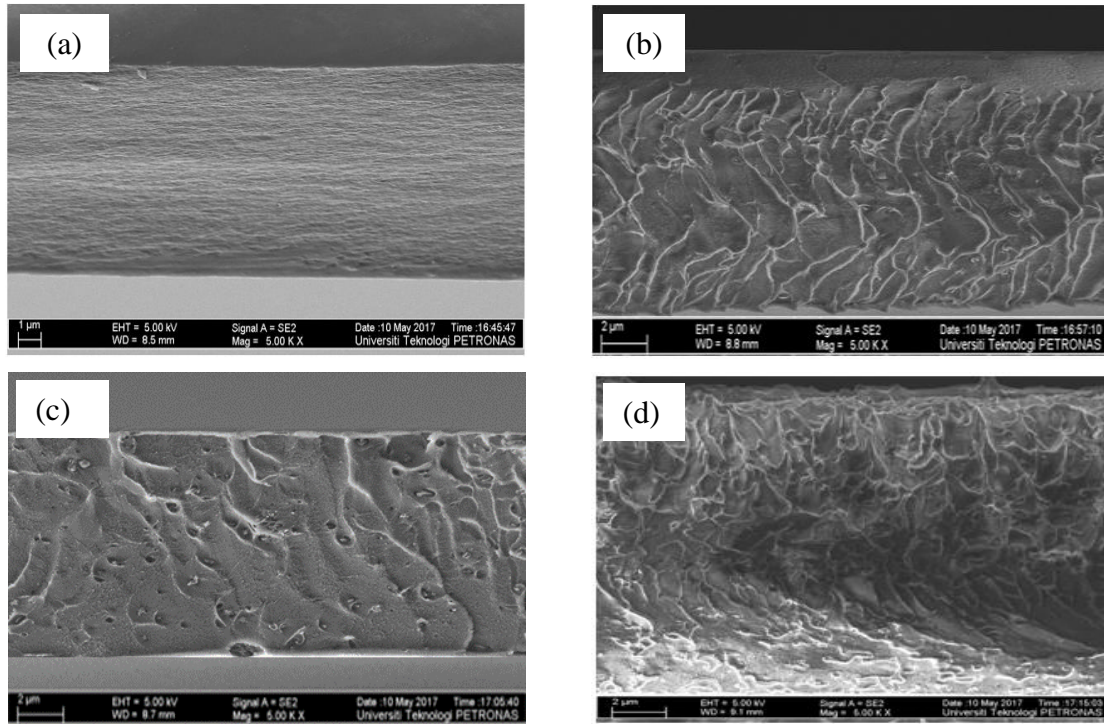


Figure 5. FESEM cross-sectional images of (a) pristine PPO_{dm} and MMM at (b) 1 wt%, (c) 3 wt% and (d) 5 wt% of CNF loading at the magnification of 5000x

Finally, the gas permeation test was carried out using pure CO₂ and CH₄ gases at fixed feed pressure 3.5 bar and room temperature condition. The CO₂ permeability and CO₂/CH₄ selectivity values of all the fabricated membranes were calculated and tabulated in Table 2. For pristine membrane, the CO₂ permeability reached 50.64 Barrer which was in good agreement with the value reported in various literatures [23, 24]. All the MMM fabricated with CNF shows increased CO₂ permeability compared to the pristine PPO_{dm} membrane. This corroborates that, the presence of CNF with larger pore diameter and smooth walls allow the gases to diffuse through it faster than the dense layer of polymer matrix [25]. Initially at 1 wt% CNF loading, approximately 80 % increment in the CO₂ gas permeability was attained and the highest CO₂ permeability, 140.71 Barrer was reported for PPO_{dm}-3 wt% CNF MMM. The addition of CNF disrupted the polymer chain packing and increased the polymer matrix free volume, resulting in improved gas permeability. On the other hand, CO₂/CH₄ ideal gas selectivity also experienced a slight enhancement after the addition of filler particles. PPO_{dm}-3 wt% CNF MMM displayed the optimum selectivity of 11.25 which was 53 % higher than the value reported for pristine PPO_{dm} membrane. These values corroborate that the gases are permeate through the membrane at different rates instead of through any undesirable voids or defect sites. Nevertheless, at 5 wt% of CNF loading the perm-selectivity values were started to reduce which might be caused by CNF agglomeration at higher filler loading on the polymer matrix. With increasing filler loading above 3 wt%, the CNF particles started to aggregate in the polymer matrix and introduces more interfacial voids which allows the gases to pass through without any discrimination.

Table 2: Perm-selectivity of pristine PPO_{dm} membrane and PPO_{dm}-CNF MMM.

| Membrane | P_{CO_2} (Barrer) | P_{CH_4} (Barrer) | α_{CO_2/CH_4} |
|-------------------------------|---------------------|---------------------|----------------------|
| Pristine PPO _{dm} | 50.64 | 6.89 | 7.35 |
| PPO _{dm} + 1 wt% CNF | 91.36 | 8.40 | 10.88 |
| PPO _{dm} + 3 wt% CNF | 140.71 | 12.50 | 11.25 |
| PPO _{dm} + 5 wt% CNF | 129.08 | 15.68 | 8.23 |

CONCLUSION

MMMs were fabricated by incorporating purified CNF at different weight loading into PPO_{dm} polymer matrix for CO₂/CH₄ gas separation application. The carbonaceous impurities have been removed from the CNF surface without leaving any defects to its morphology. At 22 wt% of PPO_{dm} the dope solution was prepared, cast and the solvent was evaporated through a series of evaporation. Upon the addition of CNF, the thermal properties of pristine PPO_{dm} membrane were improved in which higher T_d (425 °C) and T_g (210 °C) values were reported. No obvious polymer-filler interfacial defect or filler agglomeration as well as interfacial voids were observed from the cross-sectional morphology of resultant MMMs especially at 3 wt% CNF loading. The gas permeation results also exhibit noticeable enhancement in permeability and selectivity values of the membrane after the incorporation of CNF particles. Thus far, this study could be considered as the pioneer for the development of CNF-based membrane for gas separation application. Therefore, more research and detail analysis are required to explore the full potential of CNF- based MMMs in gas separation application.

ACKNOWLEDGEMENT

The authors gratefully acknowledge the financial support from Universiti Teknologi PETRONAS (UTP) under YUTP-FRG grant no. 0153AA-E08 and CO₂Centre (CO₂RES), Institute of Contaminant Management, UTP.

REFERENCES

- [1] Ismail A, Goh PS, Sanip SM, Aziz M. Transport and separation properties of carbon nanotube-mixed matrix membrane. *Separation and Purification Technology*. 2009;70(1):12-26.
- [2] Adewole J, Ahmad A, Ismail S, Leo C. Current challenges in membrane separation of CO₂ from natural gas: A review. *International Journal of Greenhouse Gas Control*. 2013;17:46-65.
- [3] Gaaz TS, Sulong AB, Akhtar MN, Raza MR. Morphology and tensile properties of thermoplastic polyurethane-halloysite nanotube nanocomposites. *International Journal of Automotive and Mechanical Engineering*. 2015;12:2845.
- [4] Pfeifer S, Bandaru P. A methodology for quantitatively characterizing the dispersion of nanostructures in polymers and composites. *Materials Research Letters*. 2014;2(3):166-75.

- [5] Dong G, Li H, Chen V. Challenges and opportunities for mixed-matrix membranes for gas separation. *Journal of Materials Chemistry A*. 2013;1(15):4610-30.
- [6] Rezakazemi M, Amooghini AE, Montazer-Rahmati MM, Ismail AF, Matsuura T. State-of-the-art membrane based CO₂ separation using mixed matrix membranes (MMMs): An overview on current status and future directions. *Progress in Polymer Science*. 2014;39(5):817-61.
- [7] Lin H, Freeman BD. Materials selection guidelines for membranes that remove CO₂ from gas mixtures. *Journal of Molecular Structure*. 2005;739(1):57-74.
- [8] Goh P, Ismail A, Sanip S, Ng B, Aziz M. Recent advances of inorganic fillers in mixed matrix membrane for gas separation. *Separation and Purification Technology*. 2011;81(3):243-64.
- [9] Othman R, Wilkinson A. The impedance characterization of hybrid cnt-silica epoxy nanocomposites. *International Journal of Automotive and Mechanical Engineering*. 2014;10:1832.
- [10] Potts JR, Dreyer DR, Bielawski CW, Ruoff RS. Graphene-based polymer nanocomposites. *Polymer*. 2011;52(1):5-25.
- [11] Skoulidas AI, Ackerman DM, Johnson JK, Sholl DS. Rapid transport of gases in carbon nanotubes. *Physical Review Letters*. 2002;89(18):185901.
- [12] Kim S, Chen L, Johnson JK, Marand E. Polysulfone and functionalized carbon nanotube mixed matrix membranes for gas separation: theory and experiment. *Journal of Membrane Science*. 2007;294(1):147-58.
- [13] Matranga C, Bockrath B, Chopra N, Hinds BJ, Andrews R. Raman spectroscopic investigation of gas interactions with an aligned multiwalled carbon nanotube membrane. *Langmuir*. 2006;22(3):1235-40.
- [14] Choi W-K, Park S-G, Takahashi H, Cho T-H. Purification of carbon nanofibers with hydrogen peroxide. *Synthetic metals*. 2003;139(1):39-42.
- [15] Li Y, Wang S, Wu H, Wang J, Jiang Z. Bioadhesion-inspired polymer-inorganic nanohybrid membranes with enhanced CO₂ capture properties. *Journal of Materials Chemistry*. 2012;22(37):19617-20.
- [16] Seno J, I N W. The uses of carbon nanotubes mixed matrix membranes (MMM) for biogas purification. *International Journal of Waste Resources (IJWR)*. 2012;2(1).
- [17] Xue Q, Pan X, Li X, Zhang J, Guo Q. Effective enhancement of gas separation performance in mixed matrix membranes using core/shell structured multi-walled carbon nanotube/graphene oxide nanoribbons. *Nanotechnology*. 2017;28(6):065702.
- [18] Yoshimune M, Fujiwara I, Haraya K. Carbon molecular sieve membranes derived from trimethylsilyl substituted poly (phenylene oxide) for gas separation. *Carbon*. 2007;45(3):553-60.
- [19] Serp P, Corrias M, Kalck P. Carbon nanotubes and nanofibers in catalysis. *Applied Catalysis A: General*. 2003;253(2):337-58.
- [20] Liu T, Tong Y, Zhang WD. Preparation and characterization of carbon nanotube/polyetherimide nanocomposite films. *Composites science and technology*. 2007;67(3):406-12.
- [21] Ismail A, Rahim N, Mustafa A, Matsuura T, Ng B, Abdullah S, et al. Gas separation performance of polyethersulfone/multi-walled carbon nanotubes

- mixed matrix membranes. *Separation and purification technology*. 2011;80(1):20-31.
- [22] Aroon M, Ismail A, Montazer-Rahmati M, Matsuura T. Effect of chitosan as a functionalization agent on the performance and separation properties of polyimide/multi-walled carbon nanotubes mixed matrix flat sheet membranes. *Journal of membrane science*. 2010;364(1):309-17.
- [23] Zhuang G-L, Tseng H-H, Wey M-Y. Preparation of PPO-silica mixed matrix membranes by in-situ sol-gel method for H₂/CO₂ separation. *International journal of hydrogen energy*. 2014;39(30):17178-90.
- [24] Hamad F, Khulbe K, Matsuura T. Comparison of gas separation performance and morphology of homogeneous and composite PPO membranes. *Journal of membrane science*. 2005;256(1):29-37.
- [25] Kim S, Pechar TW, Marand E. Poly(imide siloxane) and carbon nanotube mixed matrix membranes for gas separation. *Desalination*. 2006;192(1-3):330-9.